J Water SRT — Aqua Vol. 47, No. 1, pp. 9–20, 1998

Modeling, simulation and operational parameters of dissolved air flotation

Y. Matsui*†, K. Fukushi‡ and N. Tambo§, †*Department of Civil Engineering, Gifu University, 1-1 Yanagido, Gifu 501-11, Japan;* ‡*Department of Civil Engineering, Hachinohe Institute of Technology, 88-1 Myo, Hachinohe 031, Japan; and* §*Hokkaido University, N13W8, Sapporo 060, Japan*

ABSTRACT: This paper presents the mathematical formulation of a model for bubble–floc agglomeration in the contact zone of dissolved air flotation (DAF). It also contains rising velocity formulae for a bubble–floc agglomerate in the separation zone of DAF. The bubble–floc agglomeration model is based on the population balance of air bubbles, particles, and bubble–particle agglomerates, and the rate of bubble–floc collision and attachment. The model has been designed for two cases: where particles are larger than bubbles and vice versa. The requirements of pre-treatment (coagulation and flocculation) and the amount of air as bubbles are discussed, with the support of a model simulation. The air supply–consumption ratio (A_{sc}) is derived as an important static parameter determining DAF performance, and should be greater than 1. The traditional DAF parameter, the air–solid ratio (A_s), is proportional to the air supply–consumption ratio. The DAF model parameter evaluation suggested that it should be on the order of 0.01 or more. To ensure a sufficient bubble–floc collision rate, the DAF model simulation revealed, the kinetic parameter (bubble volume concentration times floc diameter, $\phi_b d$) should be greater than 6.0×10^{-8} m. The performance of DAF in treating a high concentration suspension (>100 mg/L) is dependent mainly on the air–solid ratio (or the air supply–consumption ratio). For low concentration suspensions ($\ll 100$ mg/L), $\phi_b d$ instead of the air–solid ratio is a dominant operational parameter in ensuring an acceptable bubble–floc collision frequency. The bubble volume concentration required for treating a low concentration suspension can be reduced with the increase of floc size by pre-flocculation.

INTRODUCTION

In water treatment, sedimentation is the most widely used pre-filtration treatment process for the production of potable water, and little attention has been devoted to any alternatives. However, water sources often contain low density particles which have a tendency to settle very slowly or to float, which poses a problem when sedimentation is used for water treatment. These difficulties have been particularly noticeable when treating low turbidity, high coloured water (containing aquatic humic substances) at low temperatures, or when removing algae from nutrient-rich stored water. Floc particles produced during the coagulation treatment of these waters have a very low density.

Consequently, the use of flotation as an alternative to gravity settling in water treatment process trains has emerged. Flotation may be defined as a process in which gases, usually air bubbles, are attached to solid particles which cause the apparent density of the resulting bubble–particle agglomerates to be less than that of water; this allows the agglomerates to rise to the surface of the liquid. In dissolved air flotation (DAF), air bubbles are produced by a reduction in water pressure when it is saturated with air.

In waste water treatment, DAF has been used extensively for the thickening of activated sludge, not only for its high separation rate, but also for the high solid content of its sludge.

In treatment for water containing algae and coloured waters, particularly in the UK and in Scandinavian countries, DAF has been used as an alternative to sedimentation prior to deep filtration. Van Vuuren *et al.* and Uden & Karlstron have reported the successful application of DAF to algal loaded water [1,2]. Following these applications, researchers at the Water Research Centre (WRc) carried out extensive work to evaluate the potential of DAF as an alternative to sedimentation in the treatment of surface waters [3–9]. They showed that recycle-flow pressure flotation is an efficient type of DAF. In this process, air is dissolved into a portion of the clarified effluent under raised pressure, and the pressurised water is then recycled and introduced to the flotation tank through a pressure releasing device and mixed with flocculated water. They also demonstrated several advantages of DAF over gravity settling:

1 Better removal is obtained for low density particles such as

*Corresponding author.

algae and flocs produced during the coagulation of coloured water;

2 A high rate of separation is expected, resulting in smaller tanks compared to sedimentation;

3 Floated sludges have a higher percentage of solids than sludges drawn from a sedimentation tank.

4 DAF can be started up quickly.

5 The chemical requirements for flotation are very similar to those of sedimentation.

6 For the efficient operation of flotation processes, flocculation into larger agglomerates (flocs) is required.

7 The quantity of air required for the treatment of surface water depends mainly on the volume of water treated rather than on the solid contents, unless the suspended concentration is very high. Whereas, for the application of DAF for waste water sludge thickening, the air/solid ratio [10] has been accepted as an important design parameter.

Recently, Edzwald *et al.* [11] developed a conceptual model that describes particle removal by DAF in water treatment. The model is based on a single collector efficiency approach where a rising air bubble is supposed to be a solid collector which is larger than the suspended particles. The steady state removal equation in their model shows that the bubble volume concentration is an important design and operating parameter. Laboratory DAF experiments conducted by Edzwald & Wingler [12], and Malley & Edzwald [13] showed that:

1 coagulation conditions of pH and coagulant dosage that produce floc particles of zero or low net charge generally produce favourable flotation conditions; and

2 the requirement of flocculation prior to DAF is analogous to direct filtration; long flocculation is not necessary prior to DAF.

Edzwald *et al.* [14,15] concluded that floc particles for DAF should be in the range of 10–30 μm and a bubble volume concentration of 4600 p.p.m. or less is sufficient to treat all waters tested. Although they discussed the design parameters based upon the conceptual model, and their preferable values for a DAF plant including pre-treatment processes (coagulation and flocculation), values for DAF parameters have not been examined for a wide range of floc size and bubble concentrations.

The goals of this paper are:

1 to present a kinetic model of DAF which is based on the population balance of air bubbles, particles, and bubble–particle agglomerates in the contact zone of bubble–particle collision-attachment;

2 to discuss the requirements of pre-treatment (coagulation and flocculation) and air bubble production; and

3 to summarise design and operation parameters.

This paper is one of two; with this paper, we present our recent results which advance the theoretical and modelling study in our previous DAF work [16–23]. Our other paper [24] deals with the application of the model to batch and pilot plant experiments.

METHODS, RESULTS AND DISCUSSION

Rising velocity of a bubble–floc agglomerate

In deriving the rising velocity formula of a bubble–floc agglomeration, two cases are considered:

1 a floc particle larger than an air bubble ($d > d_a$) and the number of air bubbles attached to a floc particle is large; and

2 a floc particle smaller than an air bubble ($d < d_a$) and the number of floc particles attached to an air bubble is large.

Rising velocity of a bubble

The falling velocity of a solid sphere for low Reynolds numbers is described by the well-known Stokes formula. The rising velocity of a bubble is, however, not determined by Stokes formula because of a change in the slipping conditions on the surface of a bubble. It is determined by the Rybczynski–Hadamard formula [25]:

$$v_a = \frac{\mathbf{g}(\rho_w - \rho_a)d_a{}^2}{6\mu} \times \frac{\mu + \mu_a}{2\mu + 3\mu_a} \tag{1}$$

Since the viscosity of water is much larger than that of air ($\mu \gg \mu_a$), the rising velocity of an air bubble is given by eqn 2:

$$v_a = \frac{\mathbf{g}(\rho_w - \rho_a)d_a{}^2}{12\mu} \tag{2}$$

Fukushi *et al.* [19] measured the rising velocities of DAF air bubbles with various sizes and confirmed the above relationship.

Rising velocity of a bubble–floc agglomerate when $\mathrm{d} > \mathrm{d_a}$

The general equation for the terminal velocity of a particle is derived by equating forces upon the particle (bubble–floc agglomerate):

$$\frac{\pi}{6} i(\rho_w - \rho_a)\mathbf{g} d_a^3 - \frac{\pi}{6}(\rho_f - \rho_w)\mathbf{g} d^3 = F_D \tag{3}$$

In DAF, a high rate of separation is expected compared to a lateral-flow sedimentation tank proceeded by a hydraulic or a mechanical flocculator (excluding upflow clarifier). A high rate of separation is achieved when the sedimentation tank is replaced by a DAF tank. This implies that the rising velocity of a bubble–floc agglomerate in a DAF tank after a flocculator is much faster than the settling velocity of a floc particle in a sedimentation tank after the flocculator. In other words, when bubbles are attached to a floc particle, the floc particle acquires a much higher speed of vertical movement than when it settles without bubbles. As a result, the buoyancy of air bubbles attached to a floc particle should be much larger in absolute value than the apparent gravity force of a floc particle in water:

$$\frac{\pi}{6} i(\rho_w - \rho_a)\mathbf{g} d_a^3 \cong \frac{\pi}{6} i\rho_w \mathbf{g} d_a^3 \gg \frac{\pi}{6}(\rho_f - \rho_w) g d^3 \tag{4}$$

Then, eqn 3 can be approximated to eqn 5:

$$\frac{\pi}{6} i\rho_w \mathbf{g} d_a^3 = F_D \tag{5}$$

The drag force (F_D) acting on a moving rigid spherical particle for low Reynolds numbers is written by:

$$F_D = 3\pi\mu d_p v \tag{6}$$

On the other hand, the drag force for a spherical bubble is represented by:

$$F_D = 2\pi\mu d_p v \tag{7}$$

The difference between these two formulae (eqns 6 and 7) is attributable to the difference in the boundary conditions of the water–particle interface and the water–bubble interface; air inside the bubble circulates, reducing the friction loss on the surface of the bubble. For a bubble–floc agglomerate, solid material attached on a bubble could retard the motion on its surface [25]. Consequently, a bubble–floc agglomerate moves (or rises) like a solid particle, supposing the no slip condition on the external surface of the agglomerate.

Then, the drag force (F_D) of the bubble–floc agglomerate is written by eqn 8, which also takes the sphericity of the agglomerate into account [26].

$$F_D = 3\pi\mu d_{fa} v \varphi^{-\frac{1}{2}} \tag{8}$$

When the number of air bubbles attached to a floc particle is large, the diameter of a bubble–floc agglomerate (d_{fa}) is given by:

$$d_{fa} = (id_a{}^3 + d^3)^{\frac{1}{3}} \tag{9}$$

Finally, substituting eqns 8 and 9 into eqn 5, the rising velocity of a bubble–floc agglomerate is written by:

$$w_{d,j} = \frac{ig\rho_w d_a^3}{18\mu d_{fa}}\varphi^{\frac{1}{2}} = \frac{ig\rho_w d_a^3}{18\mu(id_a^3 + d^3)^{\frac{1}{3}}}\varphi^{\frac{1}{2}} \tag{10}$$

Rising velocity of a bubble–floc agglomerate when $d < d_a$

The rising velocity of a bubble–floc agglomerate when the size of a floc particle is smaller than that of a bubble (and the number of floc particles attached to a bubble is large), can be derived, in the same fashion as section 2.2:

$$w_{d,i} = \frac{ig\rho_w d_a^3}{18\mu d_{af}}\varphi^{\frac{1}{2}} = \frac{g\rho_w d_a^3}{18\mu(d_a^3 + jd^3)^{\frac{1}{3}}}\varphi^{\frac{1}{2}} \tag{11}$$

Here,

$$d_{af} = (d_a{}^3 + jd^3)^{\frac{1}{3}} \tag{12}$$

Kinetics of bubble–floc agglomeration

The flotation tank of the DAF process, as illustrated in Fig. 1, is divided into two zones: a contact zone and a separation zone. In the contact zone, the flocculated water is mixed with pressurised recycled water, which is introduced through a pressure release device, in order to attach the produced air bubbles to floc particles. After the collision-attachment reaction between the air bubbles and the floc particles for the hydraulic detention time of the contact zone, bubble–floc agglomerates are produced which flow into the separation zone and rise to the surface. While quiescent flow is required in the separation zone, rather turbulent conditions are provided in the contact zone.

The collisions and attachments between bubbles and floc particles in the contact zone is a heterogeneous agglomeration process. The model of the bubble–floc agglomeration process in the contact zone comprises the rate of collision–attachment between bubbles and floc particles and the population balance of bubbles, floc particles and bubble–floc agglomerates.

Rate of bubble–floc collision

The collision frequency between bubbles and floc particles is a second order reaction, as represented by eqn 13 [18,20,21,23,25,27].

$$N = kn_a n_d \tag{13}$$

The collisions between bubbles and floc particles occur by motion in the fluid due to turbulence and to the relative motion between floc particles and bubbles due to gravity (the relative motion due to turbulence, which could be a third mechanism, is negligible because turbulent acceleration is much smaller than gravity acceleration in the fluid flow of DAF [27]). The rate of collision is written as in eqn 14, when the two types of collisions are taken into account simultaneously: collisions due to motion within turbulent fluid and collisions due to gravitational relative motion [27]:

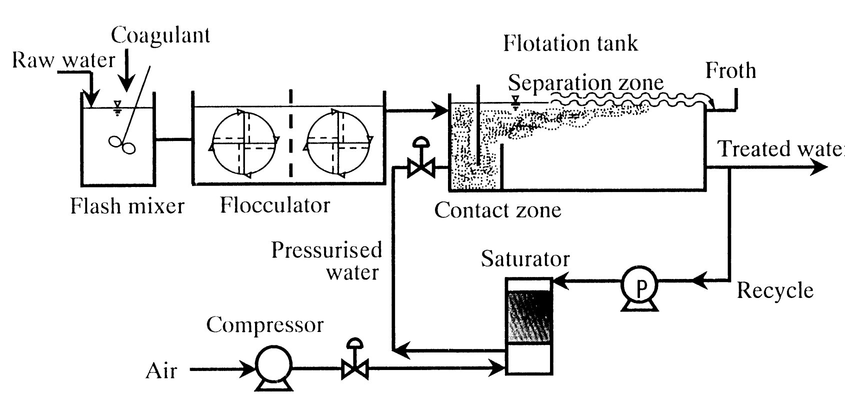

Fig. 1 Diagram of the DAF process for drinking water production.

$$k = \sqrt{k_T^2 + k_G^2} \tag{14}$$

In eqn 14, k_T is a collision rate coefficient which relates to turbulent fluid motion, and is represented by eqn 15 [25,27]:

$$k_T = aG(d_a + d)^3 = a\sqrt{\frac{\varepsilon}{\mu}}(d_u + d)^3 \tag{15}$$

According to Tambo *et al.* [28], the coefficient (a) in the equation is 0.385, whereas Suffman & Turner derive 0.209 [27].

In eqn 14, k_G is given by eqn 16 [27]:

$$k_G = \frac{1}{36}\left(\sqrt{\frac{2\pi}{3}}(d + d_a)^2\left\{(\rho_f - \rho_w)d^2 - (\rho_u - \rho_w)d_a^2\right\}\frac{g}{\mu}\right) \tag{16}$$

Since (refer to eqn 4)

$$-(\rho_a - \rho_w)d_a^2 \cong \rho_w d_a^2 > (\rho_f - \rho_w)d^2 \tag{17}$$

eqn 16 approximates to eqn 18.

$$\begin{aligned} k_G &= \frac{1}{36}\left(\sqrt{\frac{2\pi}{3}}\rho_w d_a^2 (d + d_a)^2 \frac{g}{\mu}\right) \\ &= \frac{1}{6}\left(\sqrt{\frac{2}{3\pi}}\rho_w (d + d_a)^2 \frac{g}{\mu}\left(\frac{\phi_b}{d_a}\right)\left(\frac{1}{n_a}\right)\right) \end{aligned} \tag{18}$$

If the well mixed condition is provided in the contact zone [18,19,21,23], then the collisions are predominantly brought about by particle transport by turbulent fluid motion. Then,

$$k \cong k_T \tag{19}$$

Modelling bubble–floc agglomeration when d > d$_a$

Attachment efficiency function. Every collision does not necessarily lead to the formation of a bubble–floc agglomerate. When a bubble attaches to a floc particle, thus consuming the attachment site of the floc particle, the likelihood of a successful attachment to the floc particle in the next collision decreases. Therefore, the ratio of successful collisions to all collisions (namely the attachment efficiency) is in proportion to the number of remaining attachment sites of a floc particle. In other words, the attachment efficiency decreases with increases in the number of attached bubbles, i. When initial attachment efficiency is α_0 and the maximum number of bubbles attachable to a floc particle is m_d, the attachment efficiency can be described by [18,19,21,23]:

$$\alpha_{d,i} = \alpha_0\left(1 - \frac{i}{m_d}\right) \tag{20}$$

When the number of attached bubbles i reaches m_d, no further attachment occurs. Since bubbles are attached to the surface of a floc particle, the maximum number of bubbles which can attach to a floc particle should be proportional to the surface area of the floc particle and should be inversely proportional to the square of bubble diameter: the square of bubble diameter represents the area occupied by a single bubble attached to the floc surface. Then, the maximum number of bubbles which can attach to a floc particle could be represented by [18,19,21,23]:

$$m_d = \alpha_f\left(\frac{d}{d_a}\right)^2 \tag{21}$$

Population balance model. The following assumptions were made to the population balance of bubbles, floc particles, and bubble–floc agglomerates in a contact zone:

1 The size distribution of the air bubbles is neglected. A uniform size of bubbles is assumed, because of their smaller size and their narrower size distribution than that of floc particles [19,23,24].

2 The size distribution of the floc particles has not been changed for a contact zone because of its short hydraulic duration time. Fukushi *et al.* confirmed no significant change in floc size between floc particles before and after a bubble–floc agglomeration reaction [19,23,24].

3 A coalescence between bubbles and a change in bubble size does not occur because the very strong electrical repulsive force between the bubbles [17] prevents them from attaching. According to Tambo *et al.*, no size change was observed between produced bubbles and bubbles attached to floc particles [16].

4 Many bubbles may attach to a single floc particle, however, a single bubble may not attach to more than one floc particle.

5 Bubble–floc agglomerates do not break apart.

Floc–bubble agglomerates are classified by the size of the constitutive floc particle forming them and by the number of bubbles attached to a floc particle. Namely, $n_{d,i}$ is the number concentration of floc particles of diameter d to each of which i bubbles are attached. Then, the number concentration of floc particles of size d, n_d is given by

$$n_d = \sum_{i=0}^{m_d} n_{d,i} \tag{22}$$

The total number of floc particles is given by

$$n = \int_0^{\infty} n_d \mathrm{d}d \tag{23}$$

A floc–bubble agglomerate which has i bubbles is formed by the attachment of one bubble to a floc–bubble agglomerate which has had $(i-1)$ bubbles, and it is converted to a floc–bubble agglomerate with $(i+1)$ bubbles by the attachment of another bubble. The rates of the first and second reactions are represented by $\alpha_{d,i-1}kn_a n_{d,i-1}$ and $\alpha_{d,i}kn_a n_{d,i}$ respectively: the rates of agglomeration are given by the product of the collision frequency (given by eqn 13) and attachment efficiency (given by eqn 20). Then, the population balance of floc–bubble agglomerates which have i bubbles is [18,20,21,23]:

$$\begin{aligned} \frac{\mathrm{d}n_{d,i}}{\mathrm{d}t} &= kn_a(\alpha_{d,i-1}n_{d,i-1} - \alpha_{d,i}n_{d,i}),\ i = 1 \text{ to } m_d \\ \frac{\mathrm{d}n_{d,0}}{\mathrm{d}t} &= kn_a(-\alpha_{d,0}n_{d,0}) \end{aligned} \tag{24}$$

The number of bubbles remaining can be obtained by subtracting the total number of bubbles attached on the total floc particles from the initial number of bubbles [20,21,23]:

$$n_a = n_{a,0} - \int_0^\infty \sum_{i=1}^{m_d} i n_{d,i} \, \mathrm{d}d \tag{25}$$

The analytical solution of eqns 24 and 25 can be obtained as a function of deformed time (τ) in place of real time (t) (see Appendix) [20].

$$N_{d,i} = \frac{n_{d,i}}{n_d} = \binom{m_d}{i} \exp(-K\xi)\left\{\exp\left(\frac{K\xi}{m_d}\right) - 1\right\}^{i} \tag{26}$$

$$\frac{\mathrm{d}\xi}{\mathrm{d}t} = 1 - \frac{1}{n_{a,0}} \int_0^\infty n_d m_d \left\{1 - \exp\left(-\frac{K\xi}{m_d}\right)\right\} \mathrm{d}d \tag{27}$$

$$K = k\alpha_0 n_{a,0} \tag{28}$$

The number distribution of bubbles attached to floc particles flowing into a separation zone can be obtained by solving eqns 26 and 27 and by substituting the hydraulic detention time of a contact zone into t (in DAF the duration of bubble–floc agglomeration reaction in a contact zone could be the hydraulic detention time of the contact zone, because bubbles are small enough to have a rising velocity that is much smaller than the velocity of turbulence or the bulk flow).

Simulating the variation of the number of bubbles on the floc particles. Eqns 26 and 27 give the number distribution of bubbles attached to floc particles of various sizes and the variation of this with contact time. Knowing the number of bubbles attached to a floc particle, we can calculate the velocity of rise of a bubble–floc agglomerate by the use of eqn 10. Figs 2 and 3 illustrate the velocity of rise distributions of bubble–floc agglomerates for several different contact times (deformed time, τ). The two figures are drawn under the same conditions except for floc size.

A comparison of Figs 2 and 3 shows that larger floc particles need less contact time in order to obtain the same rising velocity. For example, in Fig. 2, floc particles of 150 μm need 40 s for 50% to acquire a rising velocity of more than 0.0025 m/s. However, 300 μm floc particles need only 15 s for 50% to reach a rising speed of more than 0.003 m/s. A comparison of these two figures shows that larger floc particles attain a higher flotation speed in a shorter period of bubble–floc agglomeration reaction.

This result gives rise to the following three conclusions:

1 large floc particles do not need a long bubble–floc contact time;

2 when floc particles have a size distribution, larger floc particles reach a faster rising speed and smaller floc particles a slower rising speed after the same contact time;

3 In an extreme case in which not enough bubbles are supplied to cover the total surface of all floc particles by attachment

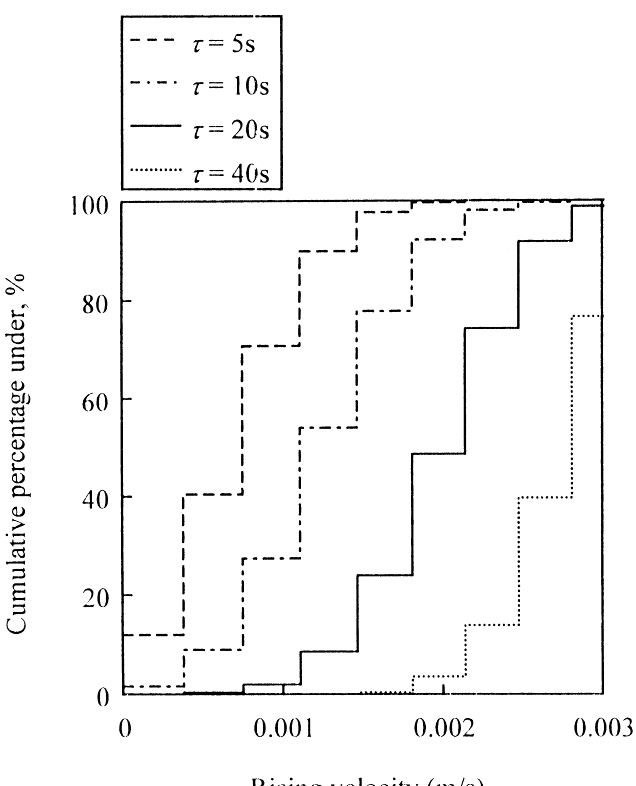

Fig. 2 Rising velocity distribution of bubble–floc agglomerates (floc diameter = 150 μm, bubble diameter = 50 μm, G = 10 /s).

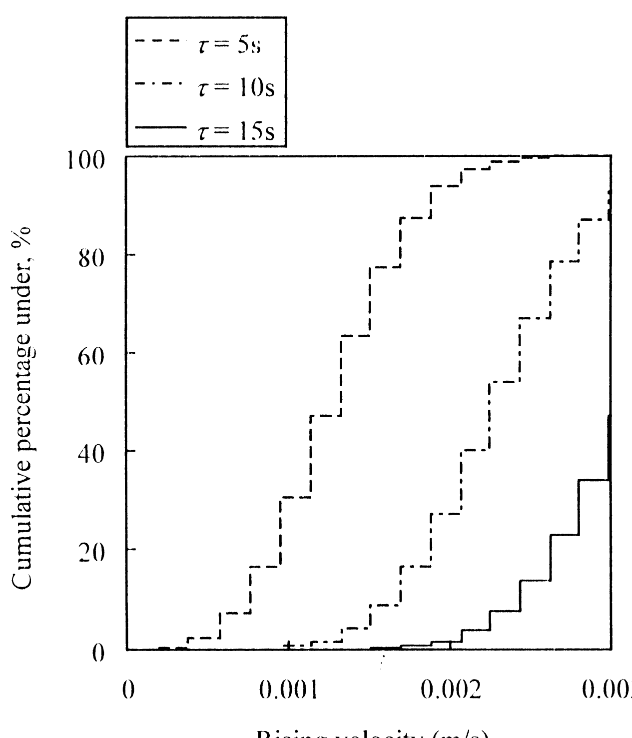

Fig. 3 Rising velocity distribution of bubble–floc agglomerates (floc diameter = 300 μm, bubble diameter = 50 μm, G = 10 /s).

(the number of produced bubbles, $n_{a,0}$, is less than the total number of attachment sites of floc particles, which is given by $\int_0^{\infty} n_d m_d \mathrm{d}d$), smaller floc particles then have a shortage of bubbles and may not have enough rising speed for separation since the bubbles are mostly consumed by larger floc particles.

In eqn 27, this condition ($n_{a,0} < \int_0^{\infty} n_d m_d \mathrm{d}d$) happens as $\mathrm{d}\tau/\mathrm{d}t = 0$, in which deformed time (τ) is limited at a certain value, and the bubble attachment reaction is terminated at that time. Finally, we understand that $n_{a,0}$ should be larger than $\int_0^{\infty} n_d m_d \mathrm{d}d$. In other words, we understand that the number of bubbles introduced into a contact zone should be enough so that a parameter A_{SC1}, defined by eqn 29 is greater than 1.

$$A_{SC1} \equiv \frac{n_{a,0}}{\int_0^{\infty} n_d m_d \mathrm{d}d} \qquad (d > d_a) \tag{29}$$

When bubbles are introduced in great excess of their consumption ($A_{SC1} \gg 1$), eqn 27 can be simplified to $\frac{d\tau}{dt} = 1$, and deformed time τ, almost equals real time t.

Modelling bubble–floc agglomeration when $d < d_a$

The kinetics of bubble–floc collision–attachment in the case where the size of floc particles is smaller than that of the bubbles will be discussed here. Assuming a uniform floc size and uniform bubble size, the reduction of floc particles by collision–attachment to bubbles is written by (the sizes of floc particles and bubbles are assumed to be unchanged because of the same reasons as discussed above)

$$\frac{\mathrm{d}n}{\mathrm{d}t} = -\alpha k n_{a,0} n \tag{30}$$

The attachment efficiency is described by eqns 31 and 32 in a similar but reverse fashion to eqns 20 and 21. Here, it is assumed that the attachment efficiency of a bubble decreases as floc particles cover the surface of the bubble.

$$\alpha = \alpha_0 \left(1 - \frac{j}{m_a}\right) \tag{31}$$

$$m_a = \alpha_a \left(\frac{d_a}{d}\right)^2 \tag{32}$$

The population balance equation for the number of floc particles is:

$$n_0 - n = j n_{a,0} \tag{33}$$

After substituting eqns 31 and 33, eqn 30 can be solved to obtain eqn 34, which gives the number concentration of floc particles remaining without attaching to any bubbles as a function of contact time t.

$$\frac{n}{n_0}\frac{1}{1 - \frac{n_0}{m_a n_{a,0}} + \frac{n}{m_a n_{a,0}}} = \exp\left[-K\left(1 - \frac{n_0}{m_a n_{a,0}}\right)t\right] \tag{34}$$

The number concentration of unattached floc particles in a separation zone can be obtained by substituting the hydraulic detention time of a contact zone into t.

When the number of introduced floc particles (n_0) is greater than the maximum available consumption by the bubble–floc attachment reaction for all bubbles ($m_a n_{a,0}$) some floc particles should remain permanently without attaching to any bubbles. Namely, when bubbles are in shortage ($\frac{m_a n_{a,0}}{n_0} < 1$), the number of floc particles that remain at $t = \infty$ is not zero ($n = n_0 - m_a n_{a,0} > 0$). This condition should be avoided in DAF, and a parameter A_{SC2}, defined by eqn 35, should be greater than 1.

$$A_{SC2} \equiv \frac{m_a n_{a,0}}{n_0} \qquad (d < d_a) \tag{35}$$

When bubbles are in great excess with respect to the bubble–floc agglomeration reaction ($A_{SC2} \equiv \frac{m_a n_{a,0}}{n_0} \gg 1$), eqn 34 can be simplified to a first order kinetic expression:

$$\frac{n}{n_0} \cong \exp(-Kt) \tag{36}$$

Requirements of bubble concentration

Air–solid ratio

Air–solid ratio and air supply–consumption ratio. The air–solid ratio (the mass ratio of introduced air over suspended solids) first proposed by Eckenfelder [10] has been widely used as an important parameter in the design and operation of DAF. In DAF for high concentration suspensions, the air–solid ratio is particularly important [9]. A theoretically grounded treatise of this parameter has not, as yet, been determined for the DAF process. However, an insight into the process might give a qualitative interpretation of the air–solid ratio. The air–solid ratio for DAF with partial recycle-flow pressure is defined as:

$$A_s = \frac{p a_m r_r}{S_s} \tag{37}$$

The air–solid ratio can be rewritten as a function of the suspended solid concentration in the contact zone (S_{sr}) and the bubble volume concentration (ϕ_b) or bubble number concentration ($n_{a,0}$):

$$A_s = \frac{\rho_a \phi_0}{S_{sr}} = \frac{\pi \rho_a n_{a,0} d_a^3}{6 S_{sr}} \tag{38}$$

On the other hand, through the discussion above and eqns 29 and 35, it is understood that the ratio of bubble supply to bubble consumption (A_{SC1} or A_{SC2}) plays an important role in bubble–floc collision–attachment and A_{SC1} (in the case where $d > d_a$) or A_{SC2} (in the case where $d < d_a$), which might be called the air supply–consumption ratio, should be greater than 1.

(a) A_S *vs.* A_{SC1} *(*$d > d_a$*).* Combining eqns 29 and 38, the relationship between A_{SC1} and the air–solid ratio A_S is derived as follows:

$$A_{SC1} = \frac{S_{sr}}{\frac{\pi}{6}\rho_a d_a^3 \int_0^{\infty} n_d m_d \mathrm{d}d} A_S \tag{39}$$

In eqn 39, the mass concentration of suspended solids (floc) is written by:

$$S_{sr} = \int_0^{\infty} \rho_p(1-\phi)\frac{\pi}{6}d^3 n_d \mathrm{d}d \quad (40)$$

The mass balance of a floc particle yields eqn 41.

$$(1-\phi)\rho_p + \phi\rho_w = \rho_{ef} + \rho_w \quad (41)$$

The buoyant density of a floc particle ρ_{ef} in eqn 41 can be written as a function of floc size [28–30]:

$$\rho_{ef} = \rho_{efo} d^{-e} \quad (42)$$

Then, the substitution of eqns 21, 40, 41 and 42 into 39 gives:

$$A_{SC1} = \frac{\rho_p \rho_{efo} \int_0^{\infty} d^{3-e} n_d \mathrm{d}d}{\alpha_f(\rho_p - \rho_w)\rho_a d_a \int_0^{\infty} d^2 n_d \mathrm{d}d} A_S \quad (43)$$

The value of the exponent e in the size–density relationship of floc particles, eqn 42, has been reported to be around 1 ($e \approx 1$) [29–33], then:

$$A_{SC1} = \frac{\rho_p \rho_{efo}}{\alpha_f(\rho_p - \rho_w)\rho_a d_a} A_S \quad (44)$$

(b) A_S *vs.* A_{SC2} *(*$d < d_a$*).* By combining eqns 35 and 38, the relationship between A_{SC2} and the air–solid ratio (A_S) is derived as follows;

$$A_{SC2} = \frac{m_a S_{sr}}{\frac{\pi}{6}\Delta\rho_a d_a^3 n_0} A_S \quad (45)$$

The mass concentration of suspended solids (floc) is written by [in the case of $d < d_a$, uniform floc size is assumed]:

$$S_{sr} = \frac{\pi}{6}\rho_p(1-\phi)d^3 n_0 \quad (46)$$

Then, substituting eqns 32, 41, 42 and 46 into 45 and assuming $e \approx 1$ [29–33], result in:

$$A_{SC2} = \frac{\alpha_a \rho_p \rho_{efo}}{(\rho_p - \rho_w)\rho_a d_a} A_S \quad (47)$$

In both eqns 44 and 47, the air–solid ratio is proportional to the air supply–consumption ratio. The requirement of the air–solid ratio could be interpreted as the necessary amount of air supplied in excess of that consumed by bubble–floc collision–attachment.

Requirements of the air–solid ratio and the A_{SC} *ratio.* From the results obtained above, the A_{SC} ratio needs to be greater than 1 for each of the cases, $d > d_a$ and $d < d_a$.

In eqns 44 or 47, the diameter of the air bubble is dependent on saturator pressure and the type of pressure-reducing nozzle, but is usually around 50×10^{-6} m [12,19,24]. We assume that the coefficient (α_f or α_a) is 1, considering the steric configuration of the attachment of bubbles on a floc particle (or the attachment of floc particles on a bubble). From the data of a size–density relationship of kaolin–aluminum flocs [33], the value of ρ_{efo} (assuming $e = 1$) was evaluated to be 0.004 kg/m^2. The densities of air bubbles and water are 1.2 kg/m^3 and 1000 kg/m^3, respectively. The density of a suspended solid particle forming clay–aluminum flocs is around 2650 kg/m^3. Substituting these values for clay–aluminum flocs, the following relationship can be derived:

$$A_S \cong 0.01\ A_{SC} \quad (48)$$

For activated sludge flocs and flocs produced during the coagulation of natural coloured water, ρ_{efo} is calculated to be $\approx$0.008 kg/m^2 [30] and 0.001 kg/m^2 [33], respectively. For activated sludge and natural-coloured-floc, we believe that the relationships between A_{SC} and A_S are similar to eqn 48, although the densities of suspended solids inside these flocs cannot be precisely quantified.

It is then understood that an air supply–consumption ratio of 1 or more implies an air–solid ratio of 0.01 or more ($A_S > 0.01$ when $A_{SC} > 1$). In other words, an operation criterion of air–solid ratios larger than 0.01 implies that air bubbles will be adequately supplied for their consumption, and that some bubbles will remain without attaching to any floc particles. The air–solid ratio was thought to be a parameter which equalizes the gravity force due to suspended solids and the buoyancy due to air bubbles. This interpretation gives an air–solid ratio of 0.001 or less [3]. According to Eckenfelder *et al.*, however, the value of the air–solid ratio is recommended to be larger than 0.02 [10]. The fact that the air–solid ratios used in practice are of the order of 0.018–0.036, greater than 0.01 [3], is compatible with our calculations of the air–solid ratio based on a discussion of the air supply–consumption ratio.

Requirement of bubble concentration and floc size

The air–solid ratio (or air supply–consumption ratio) can be regarded as a parameter which relates to an equilibrium condition of the collision–attachment reaction between air bubbles and floc particles, but it does not explain anything about how fast bubble–floc collision–attachment occurs, or the percentage of collision–attachment reactions completed in a given contact time. This would require a kinetic relationship—it might be called a kinetic requirement—in contrast to the equilibrium requirement of an air–solid ratio (or an air supply–consumption ratio).

In the results of the kinetic expression of bubble–floc agglomeration ($d > d_a$, eqn 26 and $d < d_a$, eqn 34), the rate of the reaction is related to the rate constant K ($= k\alpha_0 n_{a,0}$), for both cases. Since the rate constant (K) is a function of initial bubble concentration ($n_{a,0}$) and the floc diameter (d), we studied the relationship between them by the use of numerical simulation with eqn 26 for the case $d > d_a$ and with eqn 34 for the case $d < d_a$.

The DAF simulations were conducted under the conditions shown in Table 1. The values of the parameters substituted into eqns 26 and 34, and their related equations, are also summarised in Table 1. Since the A_S ratio should be larger than

Table 1 Input values for the DAF simulation

Removal efficiency, R	95%
Over flow rate, w_0	1/3 of rising velocity of a bubble
Air-solid ratio, A_s	$\gg 0.01$
Bubble diameter, d_a	50×10^{-6} m
Viscosity, μ	0.01 Pa.s
Contact time, t	30 s
Sphericity of bubble-floc agglomerate, φ	0.71
Mean velocity gradient in contact zone, G	10.0 s^{-1}
α_0	0.5
α_f	1.0
α_a	1.0

0.01, we assumed that $A_{SC} \gg 1$ and then $\tau \cong t$ in eqn 26. Assuming a removal efficiency at a separation zone and a contact time for agglomeration in a contact zone, the DAF simulation yields a set of relationships between initial bubble concentration and floc diameter. The DAF simulation was carried out specifically for the following procedure:

In the case d > d$_a$:

(a) The diameter of floc particles is assumed;
(b) Bubble volume concentration is assumed;
(c) The rate constant K, is calculated;
(d) The simulation of bubble–floc agglomeration by eqn 26 gives a distribution of the number of bubbles attached on the floc particles;
(e) The rising velocity distribution is calculated by eqn 10;
(f) Removal efficiency is calculated by eqn 49 (overflow rate theory);

$$R = 1 - \sum_{i=0}^{n_d} \left(1 - \frac{w_{d,i}}{w_0}\right) N_{d,i} \qquad (49)$$

(g) If the removal efficiency is not 0.95, re-assume bubble volume concentration and restart from (b);
(h) The procedure from (a) to (g) is repeated for various values of floc diameter.

In the case d < d$_a$:

(a) The diameter of floc particles is assumed;
(b) The bubble volume concentration is assumed;
(c) The rate constant K, is calculated;
(d) Simulation by eqn 34 yields the number of floc particles which have not attached to bubbles;
(e) Removal efficiency is calculated, assuming floc particles attached to a bubble are removed;
(f) If the removal efficiency is not 0.95, re-assume the bubble volume concentration and restart from (b);
(g) The procedure from (a) to (g) is repeated for various values of floc diameter.

The circles in Fig. 4 are the results of these DAF simulations. They show a relationship between floc diameter (d) and bubble volume concentration (ϕ_b, BVC), yielding 95% removal efficiency (when the coefficient of Suffman & Turner is used [27], results are slightly different, shown as triangles). For example, when the diameter of floc particles is 100 μm, the BVC should be at least 1000 p.p.m. in order to obtain a removal efficiency of 95%. The minimum BVC required can be reduced by increasing the floc size produced by flocculation, and this relationship can be roughly described by eqn 50. The line of eqn 50 is shown as the dotted line in the same figure.

$$\phi_b d = 6.0 \times 10^{-8}\,\mathrm{m} \qquad (50)$$

To ensure a sufficient bubble–floc collision rate, $\phi_b d$ should be greater than 6.0×10^{-8} m. This is a kinetic requirement which ensures sufficient collisions between bubbles and floc particles, in contrast to the equilibrium requirement ($A_S > 0.01$ or $A_{SC} \gg 1$). Good DAF performance is obtained by satisfying both requirements. With a suspended solid concentration of 100 mg/L, as in Fig. 4, the BVC should be greater than 1200 p.p.m. in order to satisfy the equilibrium requirement of the air–solid ratio, namely $A_S > 0.01$. Then, the points which satisfy both the equilibrium and kinetic requirements can be depicted as the shaded area in the figure. When the suspended solid concentration is much smaller than 100 mg/L, e.g. 10 mg/L, the minimum BVC which can satisfy an A_S of greater than 0.01 falls to 120 p.p.m., and the shaded area should be mainly enclosed by the line of $\phi_b d = 6.0 \times 10^{-8}$ m in the figure. Thus, the air–solid ratio is mainly not a parameter which determines the percentage removal for treating low concentration suspensions by DAF. The kinetics of DAF instead determine the minimum required air bubble concentration. When treating a suspension of high concentration, the bubble volume required is, however, predominantly determined by the air–solid ratio. In this case, an air–solid ratio (A_S) greater than 1 means that not only are there enough bubbles to satisfy the equilibrium requirement, but also that there are enough bubbles to ensure a sufficient rate of bubble–floc collision.

Edzwald *et al.* recommended floc particles with 10–30 μm and a BVC of 4600 p.p.m. [14,15]. Their recommendations are plotted as diamonds in the figure; they coincide well with the results of the DAF simulation. Hyde reported that a BVC of 3700–6100 p.p.m. was required for an efficient treatment of River Thames water [7].

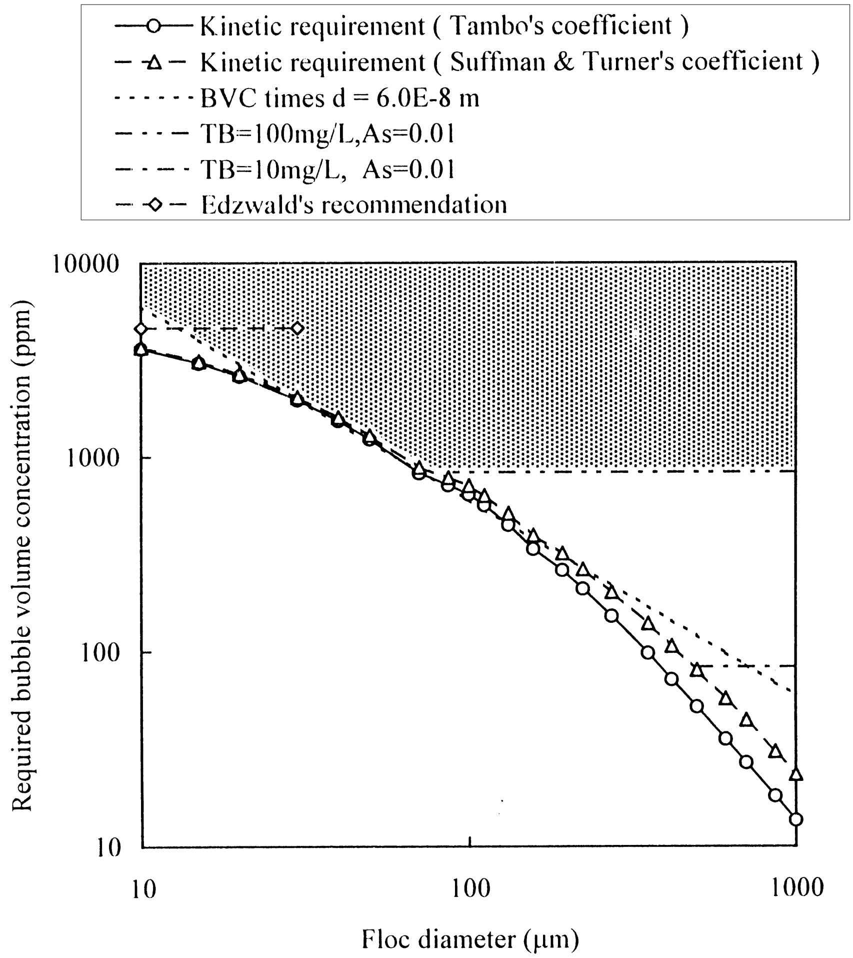

Fig. 4 Requirement of bubble volume concentration with respect to floc size.

CONCLUSION

The main points of the study are as follows.

1. Models of bubble–floc collision–attachment in the contact zone of DAF and the rising velocity of a bubble–floc agglomerate in the separation zone were proposed. The bubble–floc collision–attachment model consists of a population balance equation of floc particles, bubbles and bubble–floc agglomerates and a rate equation for bubble–floc collision and attachment. These models are derived for two cases: floc particles larger than bubbles (eqns 10, 26 and 27) and vice versa (eqns 11 and 34).

2. The air supply–consumption ratio, A_{SC1} (or A_{SC2}), is an important equilibrium parameter determining DAF performance, and should be greater than 1, based on the DAF model simulations. A traditional, but empirical DAF parameter, the air–solid ratio, is proportional to the air supply–consumption ratio. The DAF model parameter estimation revealed that the air–solid ratio is roughly 1/100 of the air supply–consumption ratio and should be of the order of 0.01 or more (equilibrium requirement).

3. To ensure a sufficient bubble–floc collision–attachment rate, the DAF model simulations revealed that the bubble volume concentration multiplied by the floc diameter, $\phi_b d$, should be greater than 6.0×10^{-8} m (kinetic requirement). The bubble volume concentration required for sufficient kinetics of bubble–floc collision–attachment can be reduced by an increase in floc size using pre-flocculation.

4. For low concentration suspensions ($\ll$100 mg/L), the bubble volume concentration multiplied by floc diameter, $\phi_b d$, is a predominant parameter determining DAF performance, in order to satisfy the bubble–floc collision–attachment frequency. However, the performance of DAF treating a high concentration suspension ($>$100 mg/L) is mainly dependent on the air–solid ratio (or air supply–consumption ratio).

5. The relationship between the equilibrium and kinetic requirements is shown in Fig. 4, in which the recommended bubble concentration and floc size are shown as a shaded area. This area satisfies the requirements of both the air–solid ratio and the value of bubble concentration multiplied by floc diameter.

ACKNOWLEDGEMENTS

We thank Mr G. Ozawa, the former head of the technical division in Hokkaido University, for his technical support; the contributions of former students of Hokkaido University and of the Hachinohe Institute of Technology, which include H. Ohta, T. Igarashi and M. Kiyotsuka, are also acknowledged.

NOMENCLATURE

- a constant (= 0.385 according to Tambo *et al.* [28] and = 0.209 according to Suffman & Turner [27]) (dimensionless)
- a_m quantity of air released per volume of water per unit pressure difference (kg/m^3/Pa)
- A_S air–solid ratio (dimensionless)
- A_{SC} ratio of supplied over consumed air bubbles in number (dimensionless)
- A_{SC1} ratio of supplied over consumed air bubbles in number when $d > d_a$ (dimensionless)
- A_{SC2} ratio of supplied over consumed air bubbles in number when $d < d_a$ (dimensionless)
- d floc diameter (m)
- d_a bubble diameter (m)
- d_p particle diameter (m)
- d_{af} diameter of a bubble–floc agglomerate when $d < d_a$ (m)
- d_{fa} diameter of a bubble–floc agglomerate when $d > d_a$ (m)
- e exponent related to size–density relationship of floc particles (dimensionless)
- F_D drag force acting on a moving particle (N)
- $\mathbf{g}$ gravitational acceleration (m/s^2)
- G velocity gradient, G value (1/s)
- i number of bubbles attached to a floc particle (dimensionless)
- i_d average number of bubbles attached to a floc particle of size d (dimensionless)
- I_d dimensionless attached bubble number (dimensionless)
- j number of floc particles attached to a bubble (dimensionless)
- k collision rate coefficient (m^3/s)
- k_T collision rate coefficient for turbulent fluid motion (m^3/s)
- k_G collision rate coefficient for differential gravitational transport (m^3/s)
- K rate constant (1/s)
- m_a maximum number of floc particles attached to a bubble, defined in eqn 32 (dimensionless)
- m_d maximum number of bubbles attached to a floc particle of size d, defined in eqn 21 (dimensionless)
- n number concentration of remaining floc particles (1/m^3)
- n_0 initial number concentration of floc particles (1/m^3)
- n_a number concentration of remaining bubble (1/m^3)
- n_d number concentration of floc particles of diameter d (1/m^3)
- $n_{a,0}$ initial number concentration of bubbles (1/m^3)
- $n_{d,i}$ number concentration of floc particles of diameter d attaching i bubbles (1/m^4)
- N collision frequency between bubbles and floc particles (1/m^3/s)
- N_a dimensionless number concentration of remaining bubbles (dimensionless)
- $N_{d,i}$ dimensionless floc number concentration (dimensionless)
- p pressure difference (Pa)
- r_r recycle ratio (dimensionless)
- R removal efficiency (dimensionless)
- S_s suspended solid (floc) concentration of influent (kg/m^3)
- S_{sr} suspended solid (floc) concentration in contact zone (kg/m^3)
- t time (s)
- v velocity of a floc particle (m/s)
- v_a rising velocity of an air bubble (m/s)
- w_o overflow rate in the separation zone (m/s)
- $w_{d,i}$ rising velocity of a bubble–floc agglomerate when $d > d_a$ (m/s)
- $w_{d,j}$ rising velocity of a bubble–floc agglomerate when $d < d_a$ (m/s)
- α attachment efficiency of bubble–floc collision (dimensionless)
- α_0 initial attachment efficiency of bubble–floc collision (dimensionless)
- α_a a coefficient (dimensionless)
- α_f a coefficient (dimensionless)
- $\alpha_{d,i}$ attachment efficiency of floc particles of diameter d attaching i bubbles (dimensionless)
- ε rate of energy dissipation per unit volume of fluid (W/m^3)
- ϕ porosity of a floc particle (dimensionless)
- ϕ_b bubble volume concentration (dimensionless)
- φ sphericity defined by Wadell, the ratio of the surface area of a sphere of the same volume as the particle to the surface of the particle (dimensionless)
- μ viscosity of water (Pa.s)
- μ_a viscosity of air (Pa.s)
- ρ_a density of air (kg/m^3)
- ρ_f density of a floc particle (kg/m^3)
- ρ_p density of suspended solids contained in a floc particle (kg/m^3)
- ρ_w density of water (kg/m^3)
- ρ_{ef} buoyant density of a floc particle (kg/m^3)
- ρ_{efo} coefficient related to size–density relationship of floc particles (kg/m^3.m^e)
- τ deformed time (s)

BIBLIOGRAPHY

1 Gregory R, Zabel TF. Sedimentation and flotation. In: AWWA. ed. *Water Quality and Treatment*, pp. 367–453. McGraw-Hill, Inc. 1990.
2 Zabel TF, Melbourne JD. Flotation. In: Lewis WM, ed. *Developments in Water Treatment–1*, pp. 139–191. Applied Science Publishers Ltd, 1980.
3 Melbourne JD, Zabel TF. *Flotation for Water and Waste Treatment*. Morlow, UK: WRc, 1977.

4 Packham RF, Richards WN. *Water Clarification by Flotation—1*. The Water Research Association, 1972.
5 Packham RF, Richards WN. *Water Clarification by Flotation—2*. The Water Research Association, 1972.
6 Packham RF, Richards WN. *Water Clarification by Flotation—3*. The Water Research Association, 1975.
7 Hyde RA. *Water Clarification by Flotation—4*. The Water Research Association, 1975.
8 Hyde RA, Miller DG, Packham RF, Richards WN. Water clarification by flotation. *JAWWA* 1977; **69**(7): 368–374.
9 Zabel T. The advantages of dissolved-air flotation for water treatment. *JAWWA* 1985; **77**(5): 42–46.
10 Eckenfelder Jr WW. *Biological Treatment of Sewage and Industrial Wastes*, Vol. 2, New York: Reinhold Pub. Co., 1958.
11 Edzwald JK, Malley Jr JP, Yu C. A conceptual model for dissolved air flotation in water treatment. *Water Supply* 1991; **9**: 141–150.
12 Edzwald JK, Wingler BJ. Chemical and physical aspects of dissolved-air flotation for the removal of algae. *J Water SRT—Aqua* 1990; **39**: 24–35.
13 Malley Jr JP, Edzwald JK. Laboratory comparison of DAF with conventional treatment. *JAWWA* 1991; **83**(9): 56–61.
14 Edzwald JK, Walsh JP, Kaminski GS, Dunn HJ. Flocculation and air requirements for dissolved air flotation. *JAWWA* 1992; **84**(3): 92–100.
15 Edzwald JK. Principles and application of dissolved-air flotation. *Water Sci Technol* 1995; **31**(3/4): 1–23.
16 Tambo N, Fukushi K, Ohta H. Comparison of flotation with sedimentation. *J Jap Water Works Assoc* 1984; **53**(12): 17–27 (in Japanese).
17 Tambo N, Igarashi T, Kiyotsuka M. An electrophoretic study of air bubble attachment to aluminium clay/color flocs. *J Jap Water Works Assoc* 1985; **54**(1): 2–6 (in Japanese).
18 Tambo N, Fukushi K. A kinetic study of dissolved air flotation. *J Jap Water Works Assoc* 1985; **54**(3): 22–30 (in Japanese).
19 Fukushi K, Tambo N, Kiyotsuka M. An experimental evaluation of kinetic process of dissolved air flotation. *J Jap Water Works Assoc* 1985; **54**(4): 32–41 (in Japanese).
20 Tambo N, Fukushi K, Matsui Y. An analysis of air bubble attachment process of dissolved air flotation. *J Jap Water Works Assoc* 1985; **54**(7): 2–11 (in Japanese).
21 Tambo N, Matsui Y, Fukushi K. A kinetic study of dissolved air flotation. *Proc World Cong III Chem Engng* Tokyo, 1986; **III**: 200–203.
22 Tambo N, Fukushi K. An evaluation of air to solid ratio by the analytical solution of bubble attachment of dissolved air flotation. *J Jap Water Works Assoc* 1987; **56**(3): 48–51 (in Japanese).
23 Fukushi K, Tambo N, Matsui Y. A kinetic model for dissolved air flotation in water and wastewater treatment. *Water Sci Technol* 1995; **31**(3/4): 37–47.
24 Fukushi K, Matsui Y, Tambo N. Experimental verification of kinetics of dissolved air flotation. *J Water SRT—Aqua*, submitted for publication.
25 Levich VG. *Physicochemical Hydrodynamics*. Prentice-Hall Inc., 1962.
26 Allen T. *Particle Size Measurement*, Vol. 1. Chapman & Hall, 1997.
27 Suffman PG, Turner JS. On the collision of drops in turbulent clouds. *J Fluid Mech* 1956; **1**: 16–30.
28 Tambo N, Hozumi H, Watanabe Y. A rational design of flocculator—I. *J Jap Water Works Assoc* 1981; **50**(6): 20–27 (in Japanese).
29 Tambo N, Watanabe Y. A study on aluminium floc density (I). *J Jap Water Works Assoc* 1967; **397**: 1–9 (in Japanese).
30 Tambo N, Watanabe Y. Physical characteristics of flocs-I. The floc density function and aluminium floc. *Water Res* 1979; **13**: 409–419.
31 Lagvanker AL, Gemmell RS. A size-density relationship for flocs. *JAWWA* 1968; **37**(9): 1040–1046.
32 Letterman RD. Flocculation. In: *Proc AWWA Seminar on Coagulation and Filtration: Back to the Basics*. AWWA, 1981.
33 Matsui Y, Tambo N. Online floc size evaluation by photometric dispersion analyzer. *Water Supply* 1990; **8**: 71–78.

APPENDIX: DERIVATION OF THE ANALYTICAL SOLUTION

Dimensionless form

On solving eqns 24 and 25, a new variable (the average number of bubbles attached to floc particles of size *d*) defined by eqn A-1 is introduced in order to obtain an auxiliary equation A-3:

$$i_d = \frac{\sum_{i=1}^{m_d} i n_{d,i}}{n_d} \tag{A-1}$$

Then, substituting eqn A-1, the mass balance equation of bubbles, eqn 25, can be rewritten by

$$n_a = n_{a,o} - \int_0^\infty i_d n_d \, \mathrm{d}d \tag{A-2}$$

Upon differentiating eqn A-2 and substituting eqn 24, eqn A-3 can be yield the rate of change of the average number of attached bubbles, i_d:

$$\frac{\mathrm{d}i_d}{\mathrm{d}t} = k n_a \alpha_{d,i_d} = k n_a \alpha_0 \left(1 - \frac{i_d}{m_d}\right) \tag{A-3}$$

The equations to solve are summarised as:

$$\frac{\mathrm{d}n_{d,i}}{\mathrm{d}t} = k n_a (\alpha_{d,i-1} n_{d,i-1} - \alpha_{d,i} n_{d,i}),\ i = 1 \text{ to } m_d$$
$$\frac{\mathrm{d}n_{d,0}}{\mathrm{d}t} = k n_a (-\alpha_{d,0} n_{d,0}) \tag{A-4}$$

$$\frac{\mathrm{d}i_d}{\mathrm{d}t} = k n_a \alpha_{d,i_d} = k n_a \alpha_0 \left(1 - \frac{i_d}{m_d}\right) \tag{A-5}$$

$$n_a = n_{a,0} - \int_0^\infty i_d n_d \, \mathrm{d}d \tag{A-6}$$

The dimensionless variables are defined as follows:

$$A_{d,i} = \frac{\alpha_{d,i}}{\alpha_0} = 1 - \frac{i}{m_d} \tag{A-7}$$

$$N_{d,i} = \frac{n_{d,i}}{n_d} \tag{A-8}$$

$$N_a = \frac{n_a}{n_{a,0}} \quad \text{(A-9)}$$

$$I = \frac{i}{m_d} \quad \text{(A-10)}$$

$$I_d = \frac{i_d}{m_d} \quad \text{(A-11)}$$

Let

$$K = k\alpha_0 n_{a,0} \quad \text{(A-12)}$$

By introducing deformed time τ, defined in eqn A-14, the derivative with respect to t is converted to the derivative with respect to τ.

$$\frac{1}{\mathrm{d}t} = \frac{1}{\mathrm{d}\tau}\frac{\mathrm{d}\tau}{\mathrm{d}t} = \frac{1}{\mathrm{d}\tau}N_a \quad \text{(A-13)}$$

$$\frac{\mathrm{d}\tau}{\mathrm{d}t} = N_a \quad \text{(A-14)}$$

Then eqns A-4, A-5 and A-6 become:

$$\frac{\mathrm{d}N_{d,i}}{\mathrm{d}\tau} = K(A_{d,i-1}N_{d,i-1} - A_{d,i}N_{d,i}),\ i = 1 \text{ to } m_d$$
$$\frac{\mathrm{d}N_{d,0}}{\mathrm{d}\tau} = K(-A_{d,0}N_{d,0}) \quad \text{(A-15)}$$

$$\frac{\mathrm{d}I_d}{\mathrm{d}\tau} = K\left(\frac{1-I_d}{m_d}\right) \quad \text{(A-16)}$$

$$N_a = 1 - \frac{1}{n_{a,0}}\int_0^1 m_d n_d I_d \,\mathrm{d}d \quad \text{(A-17)}$$

Solving eqn A-15

Let

$$\theta = K\tau \quad \text{(A-18)}$$

Eqn A-15 becomes:

$$\frac{\mathrm{d}N_{d,i}}{\mathrm{d}\theta} = A_{d,i-1}N_{d,i-1} - A_{d,i}N_{d,i},\ i = 1 \text{ to } m_d$$
$$\frac{\mathrm{d}N_{d,0}}{\mathrm{d}\theta} = (-A_{d,0}N_{d,0}) \quad \text{(A-19)}$$

Upon taking the Laplace transform of eqn A-19, the following is obtained:

$$\mathscr{L}[N_{d,i}] = \frac{1}{s+A_{d,i}}A_{d,i-1}\mathscr{L}[N_{d,i-1}] = \left(\prod_{r=0}^{i-1}A_{d,r}\right)\left(\prod_{r=0}^{i-1}\frac{1}{s+A_{d,r}}\right),\ i = 1 \text{ to } m_d \quad \text{(A-20)}$$
$$\mathscr{L}[N_{d,0}] = \frac{1}{s+A_{d,0}}$$

The corresponding functions in the time domain are:

$$N_{d,i} = \left(\prod_{r=0}^{i-1}A_{d,r}\right)\sum_{r=0}^{i}\left\{\left[\prod_{s=0,s\neq i}^{i}(A_{d,s}-A_{d,r})\right]^{-1}\exp(-A_{d,r}\theta)\right\} \quad i = 1 \text{ to } m_d$$
$$N_{d,0} = \exp(-A_{d,0}\theta) \quad \text{(A-21)}$$

As before,

$$A_{d,i} = \frac{\alpha_{d,i}}{\alpha_0} = 1 - \frac{i}{m_d} \quad \text{(A-7)}$$

Then, the groups of dimensionless parameters appearing in eqn A-21 are:

$$\prod_{r=0}^{i-1}A_{d,r} = \frac{m_d!}{m_d^i(m_d-i)!} \quad \text{(A-22)}$$

$$\prod_{s=0,s\neq i}^{i}(A_{d,s}-A_{d,r}) = \frac{m_d^i}{r!(i-r)!}(-1)^{i-r} \quad \text{(A-23)}$$

Substituting eqns A-22 and A-23 into eqn A-21 and with algebraic manipulation yields:

$$N_{d,i} = \binom{m_d}{i}\exp(-\theta)\left[\exp\left(\frac{\theta}{m_d}\right)-1\right]^i \quad \text{(A-24)}$$

Recalling the definitions of θ and $N_{d,i}$ eqn A-24 becomes:

$$N_{d,i} = \frac{n_{d,i}}{n_d} = \binom{m_d}{i}\exp(-K\tau)\left[\exp\left(\frac{K\tau}{m_d}\right)-1\right]^i \quad \text{(A-25)}$$

Solving eqns A-16 and A-17

The differential equation eqn A-16 can be solved with ease:

$$I_d = \frac{i_d}{m_d} = 1 - \exp\left(-\frac{K\tau}{m_d}\right) \quad \text{(A-26)}$$

The substitution of eqn A-26 into eqn A-17 gives the equation for a dimensionless bubble number concentration as a function of τ.

$$N_a = \frac{n_a}{n_{a,0}} = 1 - \frac{1}{n_{a,0}}\int_0^1 n_d m_d\left[1-\exp\left(-\frac{K\tau}{m_d}\right)\right]\mathrm{d}d \quad \text{(A-27)}$$

Therefore, substituting this solution into eqn A-14, the relationship between deformed time τ and real time t is obtained.

$$\frac{\mathrm{d}\tau}{\mathrm{d}t} = 1 - \frac{1}{n_{a,0}}\int_0^1 n_d m_d\left[1-\exp\left(-\frac{K\tau}{m_d}\right)\right]\mathrm{d}d \quad \text{(A-28)}$$